One-Pot Synthesis of Hierarchically Structured Ceramic Monoliths with Adjustable Porosity

Glenna L. Drisko,[†] Andrés Zelcer,[‡] Vittorio Luca,[‡] Rachel A. Caruso,*[,†,§] and
Galo J. de A. A. Soler-Illia*[,‡]

[†]*Particulate Fluids Processing Centre, School of Chemistry, The University of Melbourne, Melbourne VIC 3010, Australia,* [§]*CSIRO Materials Science and Engineering, Private Bag 33, Clayton South VIC 3169, Australia, and* [‡]*Comisión Nacional de Energía Atómica, Gerencia Quimica, Avenida General Paz 1499, San Martin, Provincia de Buenos Aires 1650, Argentina*

Received March 15, 2010. Revised Manuscript Received June 9, 2010

Hierarchically porous oxides are used in a variety of applications within the energy sector (e.g., fuel cells, batteries), biology (e.g., scaffolds, biocatalysis), separations, and catalysis. This article describes a reproducible one-step method for the preparation of metal oxides with controllable hierarchical pore architectures. The preparation is demonstrated for a wide range of materials, specifically silica, titania, zirconia, aluminum titanium oxide, titanium zirconium oxide, and yttrium zirconium oxide monoliths. The samples were prepared by exploiting the polymerization and phase separation of furfuryl alcohol to produce a colloidal dispersion of poly(furfuryl alcohol) particles. The gelation in the sol−gel process occurred after the in situ formation of the template. The removal of the polymer template led to the formation of macropores, whereas inclusion of an amphiphilic block copolymer (Pluronic F127) assisted mesopore formation, either by templating or by stabilizing the inorganic building blocks. The macropore and mesopore morphology could be altered by varying the synthesis conditions. This control over the pore structure was demonstrated in the silica, titania, and titanium zirconium oxide materials.

Introduction

Nanostructured oxides with porosity over multiple length scales are at the forefront of materials research due to the advanced functionality and enhanced reaction kinetics achieved by such systems.[1−5] Current methods for producing hierarchically porous monoliths typically require a preformed template and thus a multistep synthesis.[6−9] There is strong demand for simple and adaptable synthetic methods, such as the one reported here, where the shape, chemical composition, and pore dimensions can be adjusted according to the application. Poly(furfuryl alcohol) (PFA) is known to form a colloidal dispersion

upon cationic polymerization,[10] which can be used to template the structure of an inorganic material.

Hierarchical porosity provides high surface areas and facilitates mass transport, which can improve a material's performance in many applications.[1,11,12] We have recently tested the diffusion kinetics of macroporous and mesoporous materials and have found that the presence of large pores substantially improves mass transport.[9,13] Additionally, we found that hierarchical materials bearing an interparticulate mesopore can perform better than a material containing only a block copolymer templated mesopore.[1] Methods for producing hierarchical architectures include the use of surfactants and swelling agents[2] or supramolecular templating in conjunction with either colloidal templates,[14−17] emulsions,[18−20] vesicles, foams,[21,22]

*Corresponding author. E-mail: rcaruso@unimelb.edu.au (R.A.C.); gsoler@cnea.gov.ar (G.J.A.A.S.I.).

(1) Drisko, G. L.; Luca, V.; Sizgek, E.; Scales, N.; Caruso, R. A. *Langmuir* **2009,** *25,* 5286.
(2) Yuan, Z.-Y.; Su, B. L. *J. Mater. Chem.* **2006,** *16,* 663.
(3) Tidahy, H. L.; Siffert, S.; Lamonier, J.-F.; Zhilinskaya, E. A.; Aboukaïs, A.; Yuan, Z.-Y.; Vantomme, A.; Su, B.-L.; Canet, X.; De Weireld, G.; Frère, M.; N'Guyen, T. B.; Giraudon, J.-M.; Leclercq, G. *Appl. Catal., A* **2006,** *310,* 61.
(4) Brandhuber, D.; Torma, V.; Raab, C.; Peterlik, H.; Kulak, A.; Hüsing, N. *Chem. Mater.* **2005,** *17,* 4262.
(5) Smått, J.-H.; Weidenthaler, C.; Rosenholm, J. B.; Lindén, M. *Chem. Mater.* **2006,** *18,* 1443.
(6) Li, L.-L.; Duan, W.-T.; Yuan, Q.; Li, Z.-X.; Duan, H.-H.; Yan, C.-H. *Chem. Commun.* **2009,** 6174.
(7) Lu, A.-H.; Schüth, F. *Adv. Mater.* **2006,** *18,* 1793.
(8) Drisko, G. L.; Cao, L.; Chee Kimling, M.; Harrisson, S.; Luca, V.; Caruso, R. A. *ACS Appl. Mater. Interfaces* **2009,** *1,* 2893.
(9) Sizgek, G. D.; Griffith, C. S.; Sizgek, E.; Luca, V. *Langmuir* **2009,** *25,* 11874.
(10) Yao, J.; Wang, H.; Liu, J.; Chan, K.-Y.; Zhang, L.; Xu, N. *Carbon* **2005,** *43,* 1709.

(11) Antonietti, M.; Ozin, G. A. *Chem.—Eur. J.* **2004,** *10,* 28.
(12) Prouzet, E.; Ravaine, S.; Sanchez, C.; Backov, R. *New J. Chem.* **2008,** *32,* 1284.
(13) Sizgek, G. D.; Sizgek, E.; Griffith, C. S.; Luca, V. *Langmuir* **2008,** *24,* 12323.
(14) Doherty, C. M.; Caruso, R. A.; Smarsly, B. M.; Drummond, C. J. *Chem. Mater.* **2009,** *21,* 2895.
(15) Stein, A.; Li, F.; Denny, N. R. *Chem. Mater.* **2008,** *20,* 649.
(16) Yang, P.; Deng, T.; Zhao, D.; Feng, P.; Pine, D.; Chmelka, B.; Whitesides, G.; Stucky, G. D. *Science* **1998,** *282,* 2244.
(17) Grosso, D.; Soler-Illia, G. J. A. A.; Crepaldi, E. L.; Charleux, B.; Sanchez, C. *Adv. Funct. Mater.* **2003,** *13,* 37.
(18) Schmidt-Winkel, P.; Lukens, W. W.; Yang, P. D.; Margolese, D. I.; Lettow, J. S.; Stucky, G. D. *Chem. Mater.* **2000,** *12,* 686.
(19) Schmidt-Winkel, P.; Stucky, G. D. *Langmuir* **2000,** *16,* 356.
(20) Imhof, A.; Pine, D. J. *Nature* **1997,** *389,* 948.
(21) Chandrappa, G. T.; Steunou, N.; Livage, J. *Nature* **2002,** *416,* 702.
(22) Carn, F.; Colin, A.; Achard, M.-F.; Deleuze, H.; Sanchez, C.; Backov, R. *Adv. Mater.* **2005,** *17,* 62.

breath figures,[23] crystals of salt or water,[24,25] polymers or block copolymers,[26] or biological materials.[27] Many of these techniques involve multiple steps to produce the final structure or require expensive starting materials, therefore hindering commercialization. Phase separating templates are attracting interest in the preparation of silica and metal oxides because they can be used to produce controllable multidimensional porosity in a simple synthesis.[28−32] Moreover, this technique can be used to form monoliths,[28] thin films,[33] and very regular macroporous architectures.[34] We have recently reported a facile synthesis of hierarchically porous thin films, using a combination of phase separation and polymeric templates.[33,35]

Monoliths are the required form for many applications due to their ease of handling. For instance, in chromatographic and ion-exchange column separations, fine grain materials are unsuitable because of the build-up of back pressure. Additionally, the ability to tailor the composition of a material is necessary to achieve the broad range of physical properties desirable for advanced applications. For instance, yttrium zirconium oxides are used in fuel cells,[36−38] titania is a proven photocatalyst,[39] silica is an optimal material for column chromatography,[40] and zirconia is a common catalyst.[2] Mixed oxides can have unique chemical and physical properties and therefore can find application in many areas.[41] The Nakanishi group has pioneered polymerization-induced phase separation as a means to prepare tailorable macroporosity in monoliths of a variety of oxides, including alumina, silica, titania, and zirconia.[28−32] In one example, mesoporosity was incorporated within macroporous silica materials by aging the gel in a weakly basic solution to induce dissolution and reprecipitation.[32] Such a method has the benefit of independent macropore and mesopore control, but the drawback of an additional processing step. The Nakanishi group has also produced hierarchically porous materials using a single surfactant, however the meso- and macropore architecture cannot be independently controlled using this method.[42] Hüsing and co-workers have synthesized hierarchically porous organosilicon monoliths through a self-assembly process.[43] These monoliths have well-defined organic−inorganic domains on the nanometer scale. Generally, the approach used by these investigators involves the simultaneous phase separation of the solvent (and perhaps additives) from the inorganic sol, followed by gelation. The need to carefully control the onset and the homogeneity of both processes makes this approach very sensitive to small variations in temperature, molar ratios and other experimental conditions. This problem has been circumvented in hybrid materials by using parallel polymerizations to form interpenetrating networks of organic and inorganic polymers.[44−46] Phase separation has also been used to construct hierarchically porous zeolites.[47] In the current report, monoliths with mesopores and novel hierarchical macropore architectures arose from solvent channels and a polymer template. The synthesis of these materials was robust in that changes in temperature and humidity gave rise to similar materials with only a relatively small effect on the physical properties. The polymerization-induced phase separation occurred in advance of the gelation of the hybrid material. Thus, independent control over the meso- and macropore morphology could be achieved by adjusting the molar ratio of the templates to the silica/metal oxide precursor.

Experimental Section

Materials. Ethanol and titanium tetrachloride were purchased from Merck. FA, TEOS, Pluronic F127, zirconium(IV) chloride, aluminum isopropoxide, and yttrium isopropoxide oxide were obtained from Sigma Aldrich.

Synthesis of Titania, Zirconia, and Mixed Metal Oxide Monoliths. A 1:40 molar Ti:EtOH stock solution was prepared by dissolving $TiCl_4$ (4.49 g) in ethanol (43.60 g) while stirring (***Warning:*** *heat and HCl vapors evolve!*) and was then stored at 4 °C until used. Pluronic F127 (0.103 g, 0.0082 mmol) was dissolved in ethanol (2.6 g) and the selected metal oxide precursor solution (1.63 mmol) at 35 °C. The molar ratios, unless noted, were as follows, 1 M:0.005 Pluronic F127:2.5 FA:0.001 H_2O:40 EtOH, where M is the molar quantity of pure or mixed metals. In the mixed oxides, the molar ratios of the metals were 0.75:0.25 titanium tetrachloride:aluminum(III) isopropoxide or zirconium tetrachloride, and 0.92:0.08 zirconium tetrachloride: yttrium isopropoxide oxide. All metal oxide precursors were used as powders apart from $TiCl_4$, and ethanol was added to the individual vial to maintain a constant M:EtOH ratio. FA (0.32 g, 3.26 mmol) was added to the ethanol precursor solution and gently agitated for 15 min in closed vials. After FA addition, organic

(23) Sakatani, Y.; Boissière, C.; Grosso, D.; Nicole, L.; Soler-Illia, G. J. A. A.; Sanchez, C. *Chem. Mater.* **2008**, *20*, 1049.
(24) Gutiérrez, M. C.; Ferrer, M. L.; del Monte, F. *Chem. Mater.* **2008**, *20*, 634.
(25) Gutiérrez, M. C.; Jobbagy, M.; Rapun, N.; Ferrer, M. L.; del Monte, F. *Adv. Mater.* **2006**, *18*, 1137.
(26) Wan, Y.; Shi, Y.; Zhao, D. *Chem. Mater.* **2008**, *20*, 932.
(27) Sotiropoulou, S.; Sierra-Sastre, Y.; Mark, S. S.; Batt, C. A. *Chem. Mater.* **2008**, *20*, 821.
(28) Nakanishi, K.; Amatani, T.; Yano, S.; Kodaira, T. *Chem. Mater.* **2008**, *20*, 1108.
(29) Konishi, J.; Fujita, K.; Nakanishi, K.; Hirao, K. *Chem. Mater.* **2006**, *18*, 6069.
(30) Konishi, J.; Fujita, K.; Oiwa, S.; Nakanishi, K.; Hirao, K. *Chem. Mater.* **2008**, *20*, 2165.
(31) Nakanishi, K.; Tanaka, N. *Acc. Chem. Rev.* **2007**, *40*, 863.
(32) Nakanishi, K. *J. Sol−Gel Sci. Technol.* **2000**, *19*, 65.
(33) Fuertes, M. C.; Soler-Illia, G. J. A. A. *Chem. Mater.* **2006**, *18*, 2109.
(34) Deville, S. *Adv. Eng. Mater.* **2008**, *10*, 155.
(35) Malfatti, L.; Bellino, M. G.; Innocenzi, P.; Soler-Illia, G. J. A. A. *Chem. Mater.* **2009**, *21*, 2763.
(36) Crepaldi, E. L.; Soler-Illia, G. J. A. A.; Bouchara, A.; Grosso, D.; Durand, D.; Sanchez, C. *Angew. Chem. Int. Edn.* **2003**, *42*, 347.
(37) Mamak, M.; Coombs, N.; Ozin, G. *J. Am. Chem. Soc.* **2000**, *122*, 8932.
(38) Feng, R.; Yang, X.; Ji, W.; Au, C.-T. *Mater. Chem. Phys.* **2008**, *107*, 132.
(39) Fujishima, A.; Zhang, X.; Tryk, D. A. *Surf. Sci. Rep.* **2008**, *63*, 515.
(40) Tanaka, N.; Kobayashi, H.; Ishizuka, N.; Minakuchi, H.; Nakanishi, K.; Hosoya, K.; Ikegami, T. *J. Chromatography, A* **2002**, *965*, 35.
(41) Zou, L.; Xiang, X.; Fan, J.; Li, F. *Chem. Mater.* **2007**, *19*, 6518.
(42) Tokudome, Y.; Nakanishi, K.; Kanamori, K.; Fujita, K.; Akamatsu, H.; Hanada, T. *J. Colloid Interface Sci.* **2009**, *338*, 506.
(43) Brandhuber, D.; Peterlik, H.; Hüsing, N. *Small* **2006**, *2*, 503.
(44) Grund, S.; Kempe, P.; Baumann, G.; Seifert, A.; Spange, S. *Angew. Chem., Int. Ed.* **2006**, *46*, 628.
(45) Spange, S.; Grund, S. *Adv. Mater.* **2009**, *21*, 2111.
(46) Novak, B. M. *Adv. Mater.* **1993**, *5*, 422.
(47) Wang, H.; Pinnavaia, T. J. *Angew. Chem., Int. Ed.* **2006**, *45*, 7603.
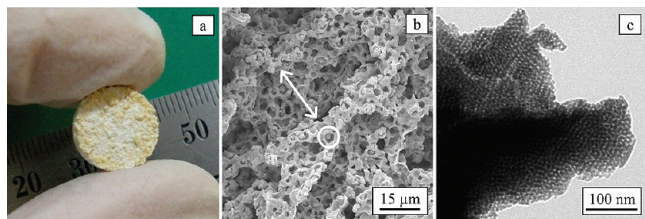
Figure 1. (a) Photograph, (b) SEM image, and (c) TEM image of a titanium zirconium oxide monolith calcined at 450 °C. The double headed arrow in (b) indicates a solvent channel; the circle a PFA-templated macrovoid.

Figure 2. Porosity in the titanium zirconium oxide monolith as seen in (a) a nitrogen sorption isotherm; (b) a mesopore size distribution based on the adsorption (black line) and desorption (gray line) branches of the nitrogen sorption isotherm; and (c) the macropore size distribution, measured using mercury porosimetry. Two peaks are observed in the macropore size distribution: 0.5−2 (due to PFA templating) and 7−13 μm (solvent channel).

polymerization occurred, which was evident because of a color change.[48] The lids were removed and replaced by punctured parafilm and the solvent was allowed to evaporate until a gel was obtained. Three independent batches were synthesized where ambient temperature varied between 16 and 33 °C and relative humidity between 21 and 83%. The solidified samples were dried further at 60−135 °C over a period of several days. The hybrid materials were calcined under a low air flow using the following program: 20 to 130 °C at a rate of 5 °C min^{-1}, 130 to 350 °C at a rate of 2 °C min^{-1}, 350 to 450 °C at a rate of 1 °C min^{-1} and held at 450 °C for 2 h.

Synthesis of Silica Monoliths. To prepare prehydrolyzed silica (PreH), tetraethyl orthosilicate (TEOS, 20.81 g), ethanol (13.81 g), and 0.138 M hydrochloric acid (1.83 g) were combined and refluxed for 2 h. The solution was allowed to cool and then stored at 4 °C in an airtight container until used. Samples were prepared as above with the following adjustments to quantities and the calcination conditions: Pluronic F127 (0.086 g) was dissolved in 5 M hydrochloric acid (0.33 g) and prehydrolyzed silica (0.50 g). Upon addition of FA (1.0 g) the solution turned dark brown. Samples were calcined under a low air flow using the following program: 30 to 130 °C at a rate of 5 °C min^{-1}, 130 to 450 at a rate of 2 °C min^{-1}, 450 to 550 °C at a rate of 1 °C min^{-1}, and held at 550 °C for 2 h.

Characterization. The surface area and pore sizes of the synthesized materials were determined by nitrogen physisorption using a Micromeritics 3000 TriStar instrument. Samples were degassed at 150 °C prior to analysis using a Micromeritics VacPrep 061. The surface area was calculated using the Brunauer−Emmett−Teller (BET) method. Pore size distributions were calculated using the Barrett−Joyner−Halenda (BJH) method from the adsorption branch.

Mercury porosimetry was used to measure the volume and pore size distribution of the macropores. Samples were degassed at 150 °C before measurement using a Micromeritics VacPrep 061 attached to a heating station. The sample was loaded into a penetrometer with a bulb size of 3 mL. The measurement was conducted on a Micromeritics AutoPore III with pressure ranging from 2 to 60 000 psi. The data were collected and analyzed using Win9420 V1.01.

Scanning electron microscopy (SEM) was performed on a FEI QUANTA 200F microscope operated at voltages between 15 and 20 kV. Samples were sliced with a scalpel, mounted on to carbon coated SEM stubs and sputter coated with a thin layer of gold using an Edwards S150B Gold Sputter Coater.

Transmission electron microscopy (TEM) analyses were conducted using a Philips CM120 BioTWIN microscope operating at 120 kV. TEM samples were prepared by finely grinding the sample in ethanol using an agate mortar and pestle, sonicating for 20 min and then drop depositing the material on to holey carbon-coated copper grids.
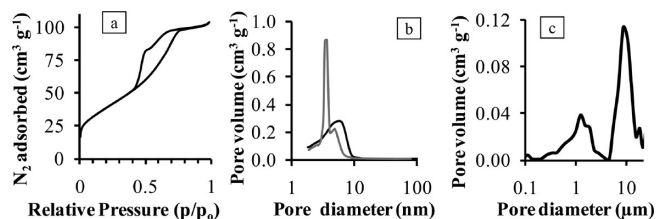
---

(48) Choura, M.; Belgacem, N. M.; Gandini, A. *Macromolecules* **1996**, *29*, 3839.

Scheme 1. Synthesis Mechanism of Hierarchically Porous Metal Oxide Monoliths: (A) polymerization of FA leads to the formation of PFA nanoparticles (depicted by black spheres) dispersed in an aqueous suspension of metal oxide/Pluronic F127/ethanol (green); (B) evaporation of ethanol and water causes the metal oxide sol to condense into a mesostructured network around the PFA particles; solvent channels (white) exist between the mesostructured metal oxide (dotted yellow); (C) calcination removes the Pluronic F127 and the PFA to leave a mesoporous and bimodal macroporous framework
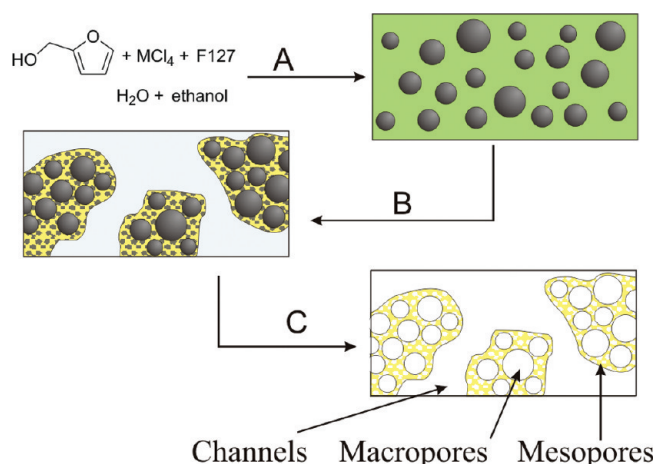
The crystallinity of the prepared materials was analyzed using X-ray diffraction (XRD). The samples were finely ground and the XRD patterns were collected from 10 to 80° 2θ on a Siemens D500 diffractometer equipped with a curved graphite crystal monochromator and a Scintag X1 diffractometer fitted with a Peltier detector. Copper K_{α} radiation at 40 kV and 30 mA was used with a step size of 0.02° 2θ and an integration time of 1 s per step. Data sets were analyzed using XPLOT for Windows (version 1.34) and the International Center for Diffraction Data Database (sets 1−54).

SAXS data was obtained on the SAXS2 line of the Laboratorio Nacional de Luz Sincrotron (The National Synchrotron Light Laboratory, LNLS), using 8 keV radiation and a bidimensional detector. Samples were ground and placed between two kapton sheets. The configuration allowed for the analysis of q spacings ranging from 0.19 to 4 nm^{-1}.

Results and Discussion

Multiscale porous cylindrical monoliths were produced by combining FA, Pluronic F127, ethanol and water with a metal oxide or silica precursor, followed by calcination.
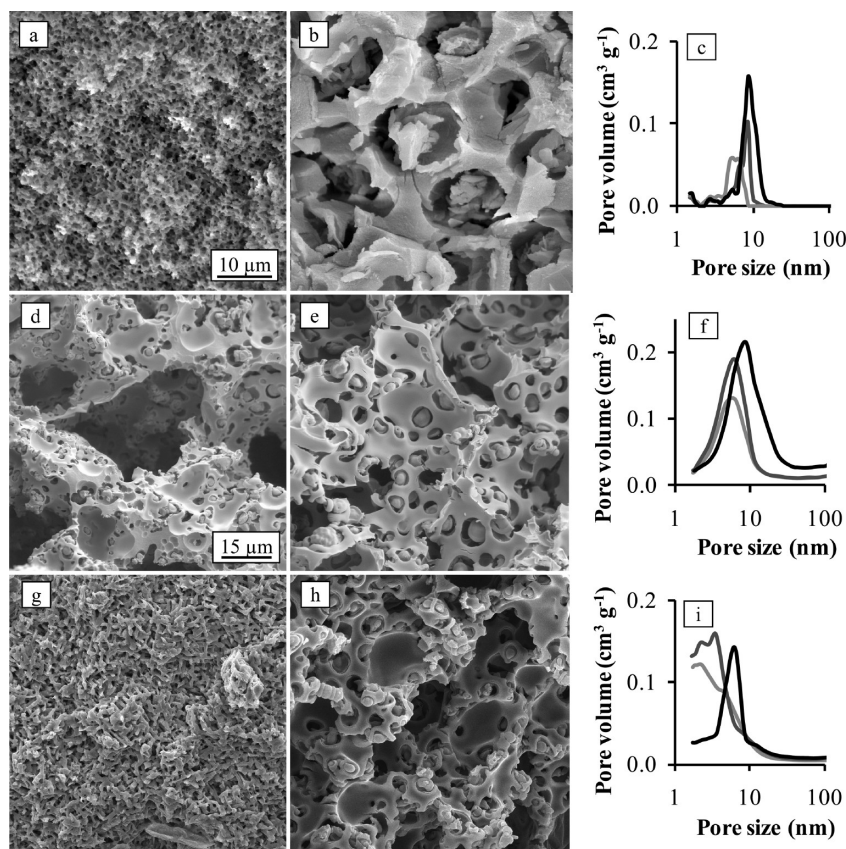
Figure 3. Size of the macropore void created in silica by PFA templating was dependent on the quantity of Pluronic F127. The amount of surfactant used per 1 mol Si was (a) 0.0025 mol Pluronic F127 and (b) 0.005 mol Pluronic F127. The scale is the same for both SEM images. (c) The mesopore size increased with increasing concentration of FA; 1 mol Si: 0.5 mol FA (gray), 1 mol FA (dark gray), and 2 mol FA (black). SEM images of titania with a ratio of 1 mol Ti to (d) 1 mol FA and (e) 2 mol FA. (f) The mesopore increased in diameter and volume with increasing ratios of Pluronic F127, specifically 0.001 mol (light gray), 0.0025 mol (dark gray), and 0.005 mol (black), relative to 1 mol Ti. SEM images of titanium zirconium oxide with a ratio of 1 mol metal to (g) 0.5 mol FA and (h) 2.5 mol FA. The scale is the same for all titania and titania zirconia SEM images. (i) The pore size distribution with varying ratios of Pluronic F127, specifically 0.001 mol (light gray line), 0.0025 mol (dark gray line), and 0.008 mol (black line), relative to 1 mol Ti + Zr. The pore size distributions were calculated using the BJH method from the nitrogen adsorption branch.

A typical example of a calcined monolith is presented in Figure 1. The monoliths shrunk 15−40% during calcination, depending on both the quantity of block copolymer and the monomer used in the preparation. The macroporosity was unique in that it consisted of a bimodal distribution of solvent channels and spherical voids derived from PFA templating. These two types of macropores are visible in the SEM image, where the width of a solvent channel is indicated with a double headed arrow and a PFA templated macrovoid is circled (Figure 1b). The TEM images of this mixed oxide material (Figure 1c) shows well formed mesopores with a significant degree of short-range order. Previously we found it to be impossible to obtain such ordered mesoporosity and compositional homogeneity in a $Ti_{1-x}Zr_xCl_4$−EtOH−H_2O−Pluronic F127 system with $x = 0.3$.[49] This does not seem to be the case here in the presence of FA and under the comparatively slow hydrolysis conditions.

The hypothesized formation mechanism for the structured materials is shown in Scheme 1. FA undergoes cationic polymerization upon initiation by protic acids

(HCl, which is either added or produced from the hydrolysis of metal chlorides)[48] and Lewis acids (e.g., metals and silicon).[50−52] PFA is immiscible in the solvent, monomer and the metal oxide precursors and therefore separates from solution to form into a particulate (colloidal) template in situ. FA polymerization is complete within the first few hours of reaction, where the gelation transition occurs later, over a number of days.[53] Initial inorganic oligomers are formed in the void spaces left by PFA, in the presence of the amphiphilic Pluronic F127, which can act in principle as a mesoporogenic agent. Hence there is no need to carefully balance the rate of the organic polymerization and the inorganic polycondensation reactions. This decoupling of the sol−gel condensation and the self-assembly processes affords multiscale texturing. As the HCl evaporates, inorganic condensation is encour-

(49) Luca, V.; Soler-Illia, G. J. A. A.; Angelome, P. C.; Steinberg, P. Y.; Drabarek, E.; Hanley, T. L. *Microporous Mesoporous Mater.* **2009**, *118*, 443.

(50) Müller, H.; Rehak, P.; Jäger, C.; Hartmann, J.; Meyer, N.; Spange, S. *Adv. Mater.* **2000**, *12*, 1671.
(51) Cesano, M. F.; Scarano, D.; Bertarione, S.; Bonino, F.; Damin, A.; Bordiga, S.; Prestipino, C.; Lamberti, C.; Zecchina, A. *J. Photochem. Photobiol., A* **2008**, *196*, 143.
(52) Zarbin, A. J. G.; Bertholdo, R.; Oliveira, M. A. F. C. *Carbon* **2002**, *40*, 2413.
(53) Grund, S.; Seifert, A.; Baumann, G.; Baumann, W.; Marx, G.; Kehr, M.; Spange, S. *Microporous Mesoporous Mater.* **2006**, *95*, 206.

aged and the metal oxide assembles around the colloidal polymer suspension, separating from the solvent and trapping the PFA template within the inorganic matrix. Calcination removes the organic matter from the hybrid material, resulting in an inorganic structure with nano- and micrometer-sized pores.

The pore architectures were assessed using nitrogen (micropore and mesopore scale) and mercury porosimetry (macropore scale). All materials demonstrated mesoporosity in the nitrogen sorption isotherms (see Figure S1 in the Supporting Information). For clarity, one example, titanium zirconium oxide, is shown in Figure 2. This material is particularly interesting because the nitrogen isotherm (Figure 2a) contains a step in the desorption branch at a relative pressure of 0.55, indicative of an open/closed mesopore system, as has been observed previously in micellar templated silica.[54] The mercury intrusion porosimetry shows that the larger pores are accessible to the liquid probe, indicating a well-connected macroporous system (Figure 2c, see Figure S2 in the Supporting Information for additional mercury porosimetry data). Channels were quantitatively measured using this technique and were found to be 5−20 μm. The spherical voids generated upon removal of the PFA from the hybrid material were 0.2−3 μm in diameter.

Pore architecture has a strong influence on the performance of materials.[1] The present templating method permits the macropore and mesopore dimensions to be easily and rationally adjusted, as is demonstrated here in the case of silica (Figure 3a−c), titania (Figure 3d−f) and titanium zirconium oxide (Figure 3g−i). The macroporous network is homogeneously and extensively interconnected (see low-magnification SEM images in Figure S3 in the Supporting Information). These oxides were produced with varying synthetic conditions to examine the adaptability of the morphology. In silica, under the conditions explored, the macropore diameter could be increased substantially by increasing the concentration of Pluronic F127. It is hypothesized that a fraction of the block copolymer acted to swell the PFA phase. Increasing FA concentration increased the dimensions of the mesopore. It can be surmised that small hydrophobic PFA oligomers formed in the early stages of sol aging are accommodated into the hydrophobic regions of the block copolymer, explaining the observed increase in mesopore size. The titania (Figure 3d,e) and titanium zirconium oxide (Figure 3g,h) synthesis conditions are necessarily much more acidic than the silica system, and thus behave quite differently. The acid concentration affects not only the condensation of the metal oxide but also the FA polymerization kinetics and probably the molecular weight of the PFA. In these materials, when the molar equivalent of FA increased, relative to the metal, the macropore size correspondingly increased. At higher concentrations of monomer the polymerization probably
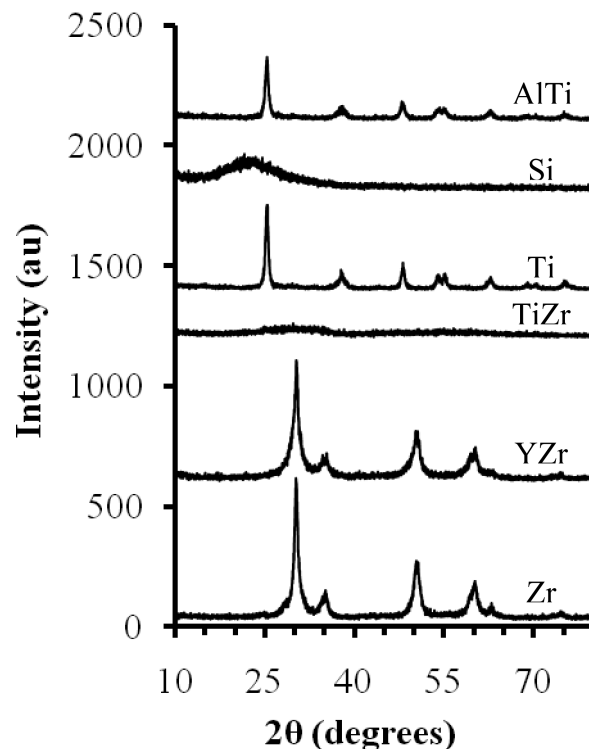

Figure 4. XRD patterns for aluminum titanium oxide (AlTi), amorphous silica (Si), titania (Ti), amorphous titanium zirconium oxide (TiZr), yttrium zirconium oxide (YZr) and zirconia (Zr). The patterns are labeled just above the corresponding plot and have been offset for comparison. All oxides were calcined at 450 °C except for Si, which was calcined at 550 °C.

reached higher molecular weight conversion, which could account for the larger macropore domains. Variation in the mesopore size distribution was observed when the molar ratio of Pluronic F127 to metal was changed (Figure 3f,i). Preliminary studies have indicated that short-range mesopore order is achievable and will be reported shortly in a full article focusing on the ideal synthesis parameters for silica (see Figure S4 in the Supporting Information).[55]

The present study demonstrates that the synthesis method is rather general and can be applied to a variety of chemical compositions. XRD of the binary oxides calcined at 450 °C showed that aluminum titanium oxide and yttrium zirconium oxide were crystalline, while the titanium zirconium oxide remained X-ray amorphous (Figure 4). Homogenously mixed titanium zirconium oxides often stay largely amorphous until well above 700 °C,[8] whereas the individual oxides in this study were already crystalline by 450 °C. To test the homogeneity of this sample, we acquired EDX measurements that showed a Ti:Zr ratio of (76 ± 1):(24 ± 1). It is likely that this synthesis could be used to produce other metal oxides or materials, such as silicon carbides,[56] or the metal oxide/PFA system could be used to produce

(54) Van Der Voort, P.; Ravikovitch, P. I.; De Jong, K. P.; Benjelloun, M.; Van Bavel, E.; Janssen, A. H.; Neimark, A. V.; Weckhuysen, B. M.; Vansant, E. F. *J. Phys. Chem. B* **2002**, *106*, 5873.

(55) Drisko, G. L.; Zelcer, A.; Caruso, R. A.; Soler-Illia, G. J. A. A. Interconnected porous silica monoliths templated by the polymerization-induced phase separation of furfuryl alcohol, in preparation.

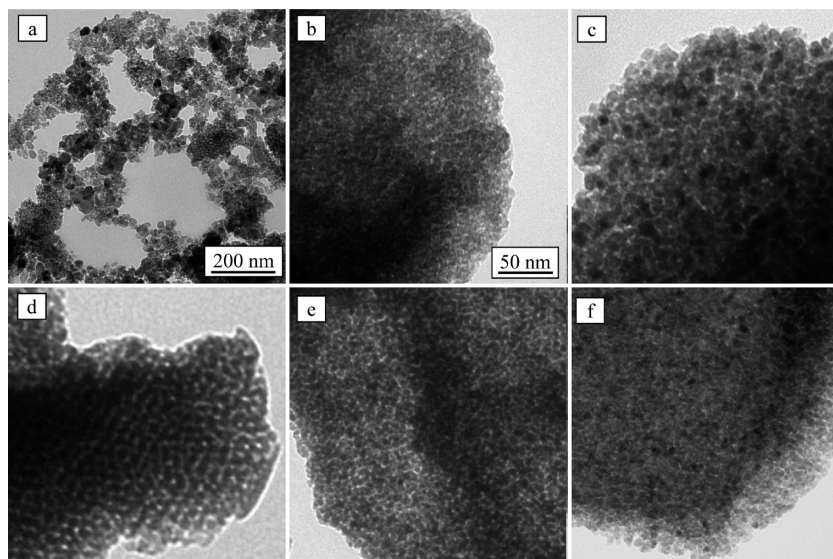(56) Wang, K.; Wang, H.; Cheng, Y.-B. *Chem. Commun.* **2010**, *46*, 303.

Figure 5. TEM images of (a) aluminum titanium oxide, (b) silica, (c) titania, (d) titanium zirconium oxide, (e) yttrium zirconium oxide and (f) zirconia after calcination. The scale is the same for b−f.

Table 1. Surface Area, Pore Volume, and Pore Size of Oxides after Calcination[a]

oxide[b]	surface area $(m^2\,g^{-1})^c$	mesopore volume $(cm^3\,g^{-1})^c$	mesopore size $(nm)^c$	macropore volume $(cm^3\,g^{-1})^d$	macropore size range $(\mu m)^d$
Si	581 ± 12	0.50 ± 0.03	3.5	2.6 ± 0.3	4−20
Ti	76 ± 15	0.10 ± 0.01	6.3	1.0 ± 0.1	0.4−3
Zr	61 ± 1	0.09 ± 0.01	4.7	1.5 ± 0.2	4−15
AlTi	180 ± 20	0.32 ± 0.03	5.0, 15.9	1.3 ± 0.1	4−20
TiZr	140 ± 7	0.16 ± 0.01	5.0	1.2 ± 0.1	0.4−20
YZr	86 ± 8	0.06 ± 0.01	4.7	0.9 ± 0.1	0.2−20

[a] Three separate batches were prepared and tested to generate the error. [b] The mixed oxides were of the molar ratio 0.25 Al:0.75 Ti, 0.75 Ti:0.25 Zr, and 0.08 Y:0.92 Zr. [c] Surface area obtained by applying BET theory to the nitrogen adsorption data. Mesopore volume determined from $p/p_o = 0.96$ on the nitrogen adsorption curve, corresponding to pores ≤ 54 nm. Mesopore size obtained from nitrogen adsorption data, size given from the peak in the pore size distribution. [d] Macropore size and volume determined from the adsorption branch of mercury intrusion porosimetry.

structured porous carbons after dissolution of the oxide framework.[57−59]

All compositions of the metal oxides investigated in this study displayed open and well-connected macroporosity (see Figure S5 in the Supporting Information for SEM images of silica, titania, zirconia, and the mixed oxides), in addition to mesoporosity (Figure 5). The mesopore structure arose from either block copolymer templating (Figure 5d) or interparticle voids between aggregated nanoparticles (textural mesoporosity, Figure 5a−c, e, and f). The Pluronic F127 is thought to be acting as a template for the mesopores and as a stabilizer for the silica nanobuilding blocks. Apart from titanium zirconium oxide, the metal oxides crystallized, forming discrete particles and losing the templated mesopore. Aluminum titanium oxide appears to contain some large crystals and some regions that retain the block copolymer templated mesopore. Bimodality is indeed observed in the nitrogen sorption pore size distribution for this sample (see Figure S1 in the Supporting Information), with the smaller

mesopore corresponding to the diameter of the titanium zirconium oxide mesopore. The silica sample remained amorphous, but demonstrated interparticle pores. This may be due to the prehydrolysis step used to prepare the silica precursor for templating. In any case, all materials contain mesopores that are of adjustable diameter and volume, as shown above.

The size of the PFA-templated macrovoids differed between oxides, probably because of differences in the acidity of the solution during polymer nucleation and growth (Table 1, see Figure S2 in the Supporting Information for mercury porosimetry data). The mesopore diameter also depended on the oxide composition (Table 1, see Figure S1 in the Supporting Information for nitrogen sorption isotherms and pore size distributions). Silica displayed the smallest mesopores, with a peak maximum at 3.5 nm, and aluminum titanium oxide had the largest mesopore showing a maximum at 15.9 nm. The large diameter of the aluminum titanium oxide is related to the large crystal size of this sample, as observed in the TEM image. Thus far, the majority of research on pore morphological control using the phase separation technique has focused on silica, as the hydrolysis and condensation reactions are easier to control.[5] The phase-separation technique described herein can be readily

(57) Almeida Filho, C.; Zarbin, A. J. G. *J. Braz. Chem. Soc.* **2006**, *17*, 1151.
(58) Almeida Filho, C.; Zarbin, A. J. G. *Carbon* **2006**, *44*, 2869.
(59) Kawashima, D.; Aihara, T.; Kobayashi, Y.; Kyotani, T.; Tomita, A. *Chem. Mater.* **2000**, *12*, 3397.

applied to an array of chemical compositions without losing the complex hierarchical pore architecture. The deviation noted in Table 1 arises from the measurements made on independent batches produced under varying environmental conditions. Ambient temperature varied from 16 to 33 °C and relative humidity between 21 and 83% between batch preparations. These changes in the synthesis conditions led to minor variations in the physical properties, suggesting that the technique is reproducible.

Hierarchical pore structure is highly relevant to the performance of materials in environmental applications, such as separations, sorption and photocatalysis;[1,60] biological applications, such as scaffolds, incorporation of large molecules, controlled drug release, avian lures and synthetic bone;[8,61] and commercial applications, such as catalysis.[62,63] Currently, the mass transport properties of the titania monoliths are being tested and the results will be published in a subsequent article. Further work will be dedicated to modifying the surfaces of these materials with organic molecules for advanced applications, such as catalytic column chromatography and selective separations.

Conclusions

A new technique for generating hierarchical pore structures in monoliths has been reported, based on exploiting differences in the polymerization rate of a monomer (FA), and the condensation rate of metal oxide precursors, in the presence of a nonionic surfactant. This technique is significantly simpler than many other syntheses because the macroporous template is readily generated in situ. Thus, pockets of reactions with different physiochemical environments were created. This partitioning permitted the development of a hybrid inorganic-surfactant phase that led to either monodisperse mesopores or to aggregated nanoparticles with textural mesoporosity. The combination of a block copolymer self-assembly and the phase separation processes induced by FA polymeriza-tion were used to provide a hierarchically porous framework in oxides of Si, Ti, Zr, AlTi, TiZr, and YZr. This diverse set of monolithic materials was prepared using the same facile one-pot procedure. The two metals in mixed titanium zirconium oxides were homogeneously dispersed, as shown by EDX.

Well-defined pores across three different length scales were obtained; pore size control was attained by adjusting the inorganic:FA:Pluronic F127 ratio. Silica, titania, and titanium zirconium oxide were used to demonstrate that the macropore and mesopore sizes could be altered by adjusting the molar equivalents of FA and Pluronic F127 relative to the metal oxide precursor. Although both mesopore and macropore dimensions could be somewhat controlled, the Pluronic F127 and PFA templating processes were not completely decoupled. Additionally, the method is robust and reproducible with variations in environmental parameters, such as temperature and humidity, resulting in only minor alterations in the physical properties. This technique satisfies the need for a robust and versatile one-pot synthesis methodology to produce structured materials with diverse compositions.

(60) Wang, X.; Yu, J. C.; Ho, C.; Hou, Y.; Fu, X. *Langmuir* **2005**, *21*, 2552.
(61) Bellino, M. G.; Tropper, I.; Duran, H.; Regazzoni, A. E.; Soler-Illia, G. J. A. A. *Small* **2010**, *6*, 1221.
(62) Xiao, F.-S.; Wang, L.; Yin, C.; Lin, K.; Di, Y.; Li, J.; Xu, R.; Su, D. S.; Schlögl, R.; Yokoi, T.; Tatsumi, T. *Angew. Chem., Int. Ed.* **2006**, *45*, 3090.
(63) Choi, M.; Cho, H. S.; Srivastava, R.; Venkatesan, C.; Choi, D.-H.; Ryoo, R. *Nat. Mater.* **2006**, *5*, 718.